Comparisons between shell and deformation dipole models for the thermal conductivity of alkali halides and its volume dependence

1989 J. Phys.: Condens. Matter 1 347

(http://iopscience.iop.org/0953-8984/1/2/003)

J. Phys.: Condens. Matter 1 (1989) 347–359. Printed in the UK

Comparisons between shell and deformation dipole models for the thermal conductivity of alkali halides and its volume dependence

Sune Pettersson†
Department of Theoretical Physics, University of Umeå, S-901 87 Umeå, Sweden

Received 6 June 1988

Abstract. Accurate dispersion relations have been used for the first time in a calculation of the volume dependence of the thermal conductivity in 16 alkali halides with the NaCl structure. Phonon dispersion relations have been calculated throughout the whole first Brillouin zone for different values of the lattice constant. These have been used to solve the Boltzmann equation by a variational method and to obtain the thermal conductivity for different lattice constants. We have used both a deformation dipole model and a shell model and we compare the results obtained with them.

We discuss various contributions to the volume dependence of the thermal conductivity and we find good agreement with room-temperature experiments. The differences in this volume dependence among the alkali halides are mainly caused by changes in the three-phonon scattering rate with volume whereas changes in the anharmonic potential give approximately the same contribution to all alkali halides studied.

1. Introduction

The volume dependence of the thermal conductivity λ is often expressed by the Bridgman parameter

$$g = -[\partial(\ln \lambda)/\partial(\ln V)]_T. \tag{1}$$

The Bridgman parameter has been measured for many alkali halides but there are very few theoretical calculations of g. The estimates that have been done start with the Leibfried–Schlömann (LS) formula [1, 2]

$$\lambda = C_1 \bar{M} \delta \theta_D^3 / n^{2/3} \gamma^2 T \tag{2}$$

where C_1 is a constant, n is the number of atoms in a primitive unit cell, θ_D is the Debye temperature, $\bar{M}$ is the mean mass of an atom, δ^3 is the volume per atom and γ is Grüneisen's parameter. The Bridgman parameter is then given by

$$g = 3\gamma + 2q - \tfrac{1}{3} \tag{3}$$

where q is the logarithmic volume derivative of γ [2]. This is a very rough way of estimating the volume dependence. The change in the frequencies ω is estimated by γ

† Present address: Solid State Division, ORNL, PO Box 2008, Oak Ridge, TN 37831, USA.

0953-8984/89/020347 + 13 $02.50

and the change in the anharmonic potential is given by q. No account is taken of the possibility that different parts of the phonon spectra behave differently when pressure is applied. This might cause some three-phonon processes to disappear while others remain relatively unchanged. Equation (3) gives fairly good agreement for many alkali halides but it cannot predict the unusually large g-values found for some alkali halides [3]. It seems as if all g-values obtained from equation (3) lie in the range 6.5–8.5 whereas experimental g-values range from 6 to 15.

In [4] the volume dependence of the mean velocity of sound and the Grüneisen parameter from models of the inter-ionic potentials were calculated. These were used in a LS-type formula to calculate the volume dependence of the thermal conductivity. It was necessary to include a structure factor to account for the decrease in the thermal conductivity across a phase change. Good agreement was found in [4] with experiments on NaCl, KCl and RbBr when the mean velocities of sound were calculated from the bulk modulus.

We have in a previous paper calculated the thermal conductivity at atmospheric pressure [5]. We used a deformation dipole (DD) model to calculate the dispersion relation throughout the whole first Brillouin zone. The linearised Boltzmann equation including only three-phonon scattering processes was solved by a variational method with a trial function $f = A\,\nabla T \cdot \boldsymbol{v}$, where $\boldsymbol{v}$ is the group velocity. We found good agreement with experiments (within 10–20%) in most crystals.

In this paper, we suggest a way to calculate the parameters in the DD model at different volumes. This makes it possible to calculate the dispersion relation and thermal conductivity at two nearby volumes and to estimate the derivative in equation (1). We use the experimentally determined room-temperature volumes at atmospheric pressure and 0.1 GPa [6]. We also employed the shell model with the parameters given in [7] and we compare the results.

2. Calculation of the dispersion relations

2.1. Shell model

The shell model parameters for the alkali halides were calculated in [7]. All parameters are ion dependent, i.e. the parameter for an ion is the same in all crystals. The only crystal-dependent parameter is the nearest-neighbour distance. The parameters have been found by simultaneously fitting the optical properties of all alkali halides. The volume dependence of the shell model parameters are found by following [8]. We assume that the shell charges, free-ion polarisabilities and ionic charges ($Z = 0.97$) are independent of volume. This means that the shell-core force constants scale with the volume. The required derivatives of the short-range potentials between nearest and next-nearest neighbours are derived from

$$\varphi_{ij}^{\mathrm{SR}}(r) = A_{ij} \exp(-\alpha_{ij} r) - C_{ij}/r^6 - D_{ij}/r^8 \qquad i, j = + \text{ or } - \tag{4}$$

with the appropriate values of r. The short-range potential includes a repulsive Born–Mayer potential and an attractive van der Waals potential. The constants A_{ij}, α_{ij}, C_{ij} and D_{ij} are determined from ion-dependent parameters [7].

With the shell model, we calculate dispersion relations for 16 alkali halides with the NaCl structure. LiI is not included since the shell model gives imaginary frequencies in this case.

2.2. Deformation dipole model

The required derivatives of the short-range potential are also in this case calculated from a potential of the form of equation (4) but we use the values of C_{ij} and D_{ij} given in [9]. The constants in the Born–Mayer part are determined from the values of the first- and second-order derivatives of the potential energy which can be derived from the elastic constants and the nearest-neighbour distance at atmospheric pressure. The values of these are taken from [10]. The elastic constants are also found in table 3 below. We include only nearest-neighbour short-range interactions since it turned out to be impossible to fit the Born–Mayer potential between next-nearest neighbours from the values of the derivatives given in [10].

The cation polarisability α_+ is assumed to be independent of volume. This assumption can be inferred from an *ab initio* calculation in [11] where the polarisability of a cation was found to be the same regardless of which crystal it was put into. In contrast, the polarisability of an anion varied greatly between different crystals. We take the cation polarisability as calculated in [11] and derive the anion polarisabilities α_- from the Clausius–Mossotti relation

$$(\varepsilon_\infty - 1/\varepsilon_\infty + 2) = (4\pi/3v_a)(\alpha_+ + \alpha_-) \tag{5}$$

where v_a is the unit-cell volume. The appropriate high-frequency dielectric constants ε_∞ to be inserted in the Clausius–Mossotti relation are taken as the experimental values at pressures of 0 and 0.1 GPa. The value at 0.1 GPa is determined from

$$(r/\varepsilon_\infty)(\mathrm{d}\varepsilon_\infty/\mathrm{d}r) = -\varepsilon_\infty(p_{11} + 2p_{12}) \tag{6}$$

where p_{11} and p_{12} are photo-elastic constants given in table 1. Note that the photo-elastic constants for the rubidium salts are not strict experimental values as explained in [15] but we include these salts in spite of this since the values seem reasonable.

The deformation dipoles which are important in this model can be simply related to the Szigeti effective charge e^* [10] which is calculated from

$$[e^*/(\mu v_a)^{1/2}]/\{1 - (4\pi/3)[(\alpha_+ + \alpha_-)/v_a]\} = [(\varepsilon_0 - \varepsilon_\infty)/4\pi]^{1/2}\omega_0 \tag{7}$$

where μ is the reduced mass of the ions, ε_0 is the static dielectric constant and ω_0 is the infrared dispersion frequency. We use the experimental values of the dielectric constants and infrared dispersion frequency which are listed in table 1. We have found experimental input data for 10 alkali halides.

3. Comparison with experiment

There are very few measurements of the dispersion relations under pressure. We have found data on only KBr, RbBr and RbI [16–18]. The Grüneisen-mode parameters

$$\gamma_{qj} = -[\![\partial\{\ln[\omega(\boldsymbol{q}, j)]\}/\partial(\ln V)]\!]_T \tag{8}$$

are given in table 2 for three different $\boldsymbol{q}$-vectors. Both models give correct sign of all Grüneisen-mode parameters and also give in most cases the correct magnitude. None of the models can be said to be better than the others from the data in table 2.

In order to check further our two models for the pressure dependence, we calculated the elastic constants from the slope of the acoustic branches in the (1, 1, 0) direction near the Γ point. It can be seen in table 3 that the shell model does not give good values

Table 1. Input values for the DD model at 0 and 0.1 GPa [11–14].

Crystal	α_+ (Å^3)	$\alpha_-(0)$ (Å^3)	p_{11}	p_{12}	$\alpha_-(0.1)$ (Å^3)	$\varepsilon_0(0)$	$\varepsilon_0(0.1)$	$\omega_{TO}(0)$ (10^{13} rad s^{-1})	$\omega_{TO}(0.1)$ (10^{13} rad s^{-1})
LiF	0.032	0.890	0.024	0.132	0.889	9.030	8.996	5.735	5.756
NaF	0.136	1.039	0.080	0.200	1.038	5.100	5.073	4.628	4.648
NaCl	0.136	3.152	0.115	0.160	3.144	5.920	5.866	3.072	3.101
NaBr	0.135	4.289	0.148	0.184	4.278	6.290	6.215	2.512	2.540
KCl	0.680	3.492	0.212	0.155	3.480	4.860	4.811	2.666	2.700
KBr	0.680	4.668	0.217	0.169	4.653	4.920	4.863	2.139	2.169
KI	0.680	6.788	0.208	0.166	6.758	5.110	5.040	1.914	1.949
RbCl	1.080	3.755	0.288	0.172	3.743	4.900	4.850	2.185	2.216
RbBr	1.080	4.960	0.293	0.185	4.943	4.870	4.813	1.642	1.673
RbI	1.080	7.064	0.262	0.167	7.030	4.930	4.864	1.419	1.447

of the elastic constants as has already been pointed out in [7]. This is especially severe in the lithium and sodium salts. The DD model gives much better elastic constants, which is expected since they have been used as input. To be more precise, we have used the bulk modulus $B = (C_{11} + 2C_{12})/3$ as input in the DD model and B^{DD} is seen to be in perfect agreement with B^{exp} as it should be. Since we are using central forces, C_{12} should be equal to C_{44}. The small differences between the model values of C_{12} and C_{44} is a measure of the accuracy of our calculated elastic constants. The better value should be that obtained for C_{44} since C_{12} is determined from a difference between terms of similar size.

The pressure dependence of the elastic constants is given in table 4 and it is seen that the shell model gives slightly better values in most cases. The pressure dependence of the elastic constant $C_{\alpha\beta}$ is given as

$$PC_{\alpha\beta} = (1/C^0_{\alpha\beta})(\Delta C_{\alpha\beta}/\Delta P) \tag{9}$$

Table 2. Comparison between the shell model, DD model and experimental values [16–18] of the Grüneisen-mode parameter γ for KBr, RbBr and RbI for three q-vectors: TA, transverse acoustic; LA, longitudinal acoustic; TO, transverse optic.

		γ_{qj}								
		(0.2, 0.0, 0.0)			(0.2, 0.2, 0.0)			(1.0, 0.0, 0.0)		
Alkali halide	Model	TA	LA	TO	TA	LA	TO	TA	LA	TO
KBr	Shell	−0.40	2.53	2.54	−0.35	1.83	2.43	−0.61	−0.25	2.70
KBr	DD	−0.67	2.37	2.36	−0.59	1.55	2.28	−0.84	−0.24	2.45
KBr	Experimental	−0.70	2.50	—	−0.60	2.30	—	−0.70	−0.60	—
RbBr	Shell	−0.73	2.51	2.45	−0.66	1.84	2.34	−1.03	−0.61	2.64
RbBr	DD	−0.76	2.35	2.10	−0.68	1.58	2.06	−1.07	−0.65	2.19
RbBr	Experimental	−0.46	2.53	—	−0.86	1.60	—	−0.84	−0.67	—
RbI	Shell	−0.62	2.49	2.44	−0.57	1.87	2.34	−0.97	−0.67	2.64
RbI	DD	−0.82	2.39	2.36	−0.74	1.61	2.27	−1.12	−0.65	2.51
RbI	Experimental	−0.98	1.84	2.30	−1.28	1.89	2.40	−1.53	−0.84	2.46

Table 3. Elastic constants at 300 K calculated with the shell model and DD model compared with experimental values [10].

Crystal	C_{11}^{shell} (10^{10} Pa)	C_{11}^{DD} (10^{10} Pa)	C_{11}^{exp} (10^{10} Pa)	C_{12}^{shell} (10^{10} Pa)	C_{12}^{DD} (10^{10} Pa)	C_{12}^{exp} (10^{10} Pa)	C_{44}^{shell} (10^{10} Pa)	C_{44}^{DD} (10^{10} Pa)	C_{44}^{exp} (10^{10} Pa)
LiF	19.3	9.8	11.1	11.1	5.0	4.2	11.5	4.9	6.3
LiCl	7.1	—	4.8	3.9	—	1.9	4.0	—	2.5
LiBr	5.7	—	3.9	3.1	—	1.9	3.2	—	1.9
NaF	12.6	9.0	9.6	3.2	2.8	2.5	3.4	2.8	2.8
NaCl	6.2	5.0	4.9	1.8	1.3	1.3	1.9	1.3	1.3
NaBr	5.3	4.0	4.0	1.6	1.0	1.0	1.6	1.0	1.0
NaI	3.9	—	3.0	1.2	—	0.9	1.2	—	0.7
KF	7.6	—	6.5	1.3	—	1.6	1.4	—	1.2
KCl	4.7	3.9	4.1	0.82	0.83	0.71	0.87	0.82	0.63
KBr	4.2	3.3	3.5	0.73	0.69	0.58	0.74	0.68	0.51
KI	3.4	2.6	2.7	0.61	0.53	0.45	0.61	0.52	0.36
RbF	6.1	—	5.5	0.95	—	1.40	0.99	—	0.92
RbCl	4.1	3.6	3.7	0.60	0.69	0.64	0.64	0.68	0.48
RbBr	3.7	3.0	3.2	0.53	0.58	0.47	0.55	0.57	0.38
RbI	3.1	2.5	2.6	0.46	0.45	0.38	0.45	0.44	0.28
CsF	4.8	—	5.1	0.61	—	1.24	0.58	—	0.78

Table 4. Pressure dependence of the elastic constants obtained with the shell model and DD model compared with experimental values [12]: $PC_{11} = (1/C_{11}^0)\Delta C_{11}/\Delta P$, etc.

Crystal	PC_{11}^{shell} (10^{-10} Pa^{-1})	PC_{11}^{DD} (10^{-10} Pa^{-1})	PC_{11}^{exp} (10^{-10} Pa^{-1})	PC_{12}^{shell} (10^{-10} Pa^{-1})	PC_{12}^{DD} (10^{-10} Pa^{-1})	PC_{12}^{exp} (10^{-10} Pa^{-1})	PC_{44}^{shell} (10^{-10} Pa^{-1})	PC_{44}^{DD} (10^{-10} Pa^{-1})	PC_{44}^{exp} (10^{-10} Pa^{-1})
LiF	1.1	0.7	0.9	0.7	0.4	0.6	0.32	−0.01	0.22
LiCl	2.2	—	2.2	1.3	—	1.4	0.49	—	0.68
LiBr	2.7	—	2.8	1.7	—	1.6	0.65	—	0.88
NaF	1.2	1.0	1.3	0.9	0.6	1.0	0.08	−0.09	0.10
NaCl	2.6	2.2	2.5	1.9	1.4	1.8	0.32	−0.28	0.29
NaBr	2.8	2.4	3.0	2.2	1.6	2.0	0.43	−0.33	0.46
NaI	3.9	—	4.1	3.0	—	2.9	0.71	—	0.80
KF	3.2	—	1.9	2.5	—	1.2	−0.71	—	−0.34
KCl	3.0	2.8	3.0	2.5	1.9	1.4	−0.31	−0.59	−0.75
KBr	3.3	3.0	3.8	2.9	2.2	2.9	−0.25	−0.59	−0.64
KI	4.2	4.0	4.8	3.9	2.9	3.6	−0.10	−0.83	−0.61
RbF	1.9	—	2.2	1.5	—	1.6	−0.63	—	−0.76
RbCl	3.5	3.3	4.0	3.0	2.4	2.8	−0.76	−0.73	−1.32
RbBr	4.1	3.8	4.5	3.8	2.8	3.8	−0.82	−0.84	−1.54
RbI	5.1	4.8	5.4	4.9	3.6	3.4	−0.80	−1.18	−1.83
CsF	1.9	—	—	1.6	—	—	−1.28	—	—

Table 5. The TO frequency at the Γ point and its mode γ calculated with the shell model and DD model compared with experimental values [14, 19–22].

Crystal	ω_{TO}^{shell} (10^{13} rad s^{-1})	ω_{TO}^{DD} (10^{13} rad s^{-1})	ω_{TO}^{exp} (10^{13} rad s^{-1})	γ_{TO}^{shell}	γ_{TO}^{DD}	γ_{TO}^{exp}
LiF	5.22	5.80	5.76	6.17	1.58	2.35, 2.59
LiCl	3.39	—	3.81	7.31	—	—
LiBr	2.80	—	3.22	7.84	—	—
NaF	4.57	4.44	4.64	2.62	2.55	2.08, 2.95
NaCl	3.04	3.23	3.08	3.15	2.31	2.35, 2.31
NaBr	2.51	2.64	2.52	3.11	2.50	2.37, 2.58
NaI	2.07	—	2.18	3.37	—	2.54
KF	3.55	—	3.57	2.42	—	—
KCl	2.64	2.57	2.67	2.60	2.27	2.28, 2.83, 2.20
KBr	2.14	2.08	2.14	2.52	2.35	2.06, 2.46, 2.30
KI	1.86	1.79	1.92	2.56	2.39	2.20, 3.1, 2.14
RbF	2.85	—	2.94	2.35	—	—
RbCl	2.16	2.18	2.24	2.51	2.32	2.16, 2.40
RbBr	1.64	1.60	1.69	2.43	2.09	2.39, 2.02
RbI	1.41	1.36	1.41	2.41	2.34	2.09, 2.5, 2.38
CsF	2.43	—	2.39	2.15	—	—

It is only PC_{44} for the potassium and rubidium salts that are better given by the DD model but it cannot reproduce the change in sign of PC_{44} when going towards the lighter alkali halides.

Table 6. The linear coefficient α_l, of thermal expansion and the specific heat C_V per unit cell at 300 K calculated with the shell model and DD model compared with experimental values [23, 24].

Crystal	α_l^{shell} ($10^{-5}K^{-1}$)	α_l^{DD} (10^{-5} K^{-1})	α_l^{exp} (10^{-5} K^{-1})	C_V^{shell} (10^{-23} J K^{-1})	C_V^{DD} (10^{-23} J K^{-1})	C_V^{exp} (10^{-23} J K^{-1})
LiF	5.87	2.21	3.44	6.50	6.67	6.47
LiCl	8.56	—	4.40	7.58	—	7.30
LiBr	8.42	—	4.89	7.82	—	7.50
NaF	3.44	3.03	3.35	7.43	7.50	7.49
NaCl	4.48	3.26	4.02	7.89	7.90	7.90
NaBr	4.73	3.64	4.18	8.03	8.03	8.01
NaI	4.89	—	4.48	8.10	—	8.07
KF	3.08	—	3.14	7.81	—	7.78
KCl	3.85	3.30	3.66	8.03	8.04	8.04
KBr	3.92	3.48	3.85	8.11	8.12	8.13
KI	4.19	3.67	4.04	8.15	8.16	8.16
RbF	2.88	—	3.17	7.97	—	7.90
RbCl	3.59	3.28	3.66	8.11	8.11	8.11
RbBr	3.74	3.21	3.77	8.18	8.18	8.19
RbI	3.87	3.55	3.93	8.20	8.20	8.22
CsF	1.90	—	3.17	8.05	—	7.94

We have also checked the value of the TO frequency at the Γ point. The shell model gives a slightly better value of the frequency while the DD model gives a better volume dependence (table 5). The shell model values of ω_{TO} were expected to be close to the experimentally determined ω_{TO} since these have been used in the fitting procedure.

As a control of the average behaviour of all phonons, we calculated the linear coefficient α_l of thermal expansion and the heat capacity G_V per unit cell at 300 K from the relations

$$\alpha_l(T) = \frac{1}{3B}\sum_{qj}\gamma_{qj}C_{qj}(T) \tag{10}$$

$$C_V(T) = \sum_{qj} C_{qj}(T) \tag{11}$$

$$C_{qj}(T) = \{[\hbar\omega(\boldsymbol{q},j)]^2/kT^2\}N_0(\boldsymbol{q},j)[N_0(\boldsymbol{q},j)+1]. \tag{12}$$

The general trend in table 6 is that the DD model in all cases gives too low a value of α_l whereas the shell model gives too high a value of α_l in most crystals. Once again the lithium salts are well off the mark but in the other salts the agreement is within 10–20% with the DD model and within 1–10% with the shell model. The C_V-values obtained with both models are in very good agreement with experiments with the exception of the lithium salts.

From all these controls of the dispersion relations, it is not possible to say that one model is better than the other. The severe failure of the shell model is that it does not give the initial slope of the acoustic branches correctly. In contrast, the shell model gives good values for most volume dependences of the frequencies. It is clear, however, that none of the models works well for the lithium salts.

Table 7. The thermal conductivity λ at 300 K calculated with the shell model and DD model compared with experimental values. C_{111} is a third-order derivative of the potential energy of a pair of nearest neighbours.

Crystal	λ^{shell} ($W\,m^{-1}\,K^{-1}$)	C_{111}^{shell} (10^{12} Pa)	λ^{DD} ($W\,m^{-1}\,K^{-1}$)	C_{111}^{DD} (10^{12} Pa)	λ^{exp} ($W\,m^{-1}\,K^{-1}$)	Reference
LiF	8.30	−2.38	13.92	−1.01	14.30	[25]
LiCl	1.08	−0.96	—	—	—	
LiBr	0.591	−0.71	—	—	1.80	[26]
NaF	14.3	−1.67	21.2	−1.07	16.3	[27]
NaCl	5.28	−0.84	6.32	−0.63	5.95	[28]
NaBr	1.56	−0.67	2.10	−0.50	2.15	[29]
NaI	0.523	−0.48	—	—	1.30	[28]
KF	4.90	−1.02	—	—	6.35	[30]
KCl	6.61	−0.66	6.49	−0.51	6.17	[31]
KBr	2.81	−0.56	2.54	−0.43	2.75	[31]
KI	1.66	−0.45	1.41	−0.34	1.91	[31]
RbF	1.03	−0.80	—	—	2.25	[26]
RbCl	2.06	−0.58	2.23	−0.49	2.33	[31]
RbBr	4.18	−0.50	4.05	−0.39	3.23	[31]
RbI	2.66	−0.42	2.19	−0.32	1.93	[31]
CsF	0.759	−0.58	—	—	—	

4. The thermal conductivity

The expression obtained for the thermal conductivity in [5] is

$$\lambda = T\theta^2/G \tag{13}$$

where θ and G are two integrals given in [5]. The scattering processes are found in the integral G whereas θ is proportional to a summation over the heat carried by each branch.

The calculated thermal conductivity at 300 K is found in table 7 together with experimental data and values of the third-order derivatives C_{111} of the potential energy of a pair of nearest neighbours, which have been used in the calculations. As we already mentioned in § 2.2, we were able to calculate dispersion relations with the DD model for only 10 crystals. The DD model gives a thermal conductivity higher than that obtained with the shell model in the lithium and sodium salts and in RbCl. This difference can be explained by the magnitudes of C_{111} which are smaller with the DD model than with the shell model in all alkali halides. However, this cannot explain the reverse relationship of the calculated λ-values for RbBr, RbI and the potassium salts which has to be explained by differences in the calculated dispersion relations.

As we pointed out in [5], the value of C_{111} is very sensitive to the parameters in the assumed potential. We have in this paper also included van der Waals potentials; this results in a lower value of the magnitude of C_{111}. This leads in some cases to calculated λ-values which are higher than the experimental values. According to the variational principle, we should always obtain a lower estimate of the thermal conductivity, indicating that some part of our model is not entirely correct.

The most probable cause of the discrepancies is the value of C_{111} since it varies greatly with different models for the potential energy. We have also noted that the inclusion of van der Waals potentials increases the magnitude of the third-order derivatives of the potential energy of a pair of next-nearest neighbours. When account is taken of the fact that there are more terms coming from the summation over next-nearest neighbours than from the summation over nearest neighbours, we can expect an additional contribution of several per cent if next-nearest neighbours are included in the anharmonic coupling. Whether this would give a higher or lower value of the thermal conductivity is not certain.

The largest changes in the λ^{DD}-values compared with our previous calculation with the DD model [5] are found for RbBr and RbI. The previous small λ^{DD}-value for RbI has now increased and gives rather good agreement with experiment while the λ^{DD}-value of RbBr is now severely overestimated. The extremely low λ^{DD}-value for KI found previously has improved somewhat but it is still too low. Apparently, KI must have some properties which are difficult to include in simple theories since also in a phenomenological examination of measured thermal conductivity values [32] KI did not fit into the theory.

5. Volume dependence of the thermal conductivity

In order to find the important contributions to g (equation (1)), we extract the explicit r-dependence from the integrals in equation (13) (including the r-dependences in $\boldsymbol{q}$ and $\boldsymbol{v}$) and we obtain $\theta = r^2\theta_{res}$ and $G = r^5 C_{111}^2 G_{res}$ where C_{111} is a third-order derivative of

Table 8. Calculated Bridgman parameter g according to equation (14) and experimental g-values at 300 K. The upper rows for each alkali halide are the shell model results and the lower rows the DD model results.

Crystal	g_{exp}	Reference	g	Contributions to g from each term in equation (14)			
				$\frac{1}{3}$	$-\frac{2}{3}\partial(\ln\theta_{res})/\partial(\ln r)$	$+\frac{2}{3}\partial(\ln C_{111})/\partial(\ln r)$	$+\frac{1}{3}\partial(\ln G_{res})/\partial(\ln r)$
LiF	7.9	[25]	12.4	0.3	−4.9	−10.4	27.4
			4.8	0.3	−1.9	−5.8	12.2
LiCl	—		8.2	0.3	−9.3	−10.5	27.7
			—	—	—	—	—
LiBr	7.0	[26]	6.0	0.3	−17.7	−10.2	33.6
			—	—	—	—	—
NaF	7.6	[27]	11.6	0.3	4.3	−7.7	14.7
			7.7	0.3	4.9	−6.4	8.9
NaCl	7.4	[28]	11.7	0.3	4.5	−8.3	15.2
			7.8	0.3	4.6	−6.9	9.7
NaBr	9.7	[29]	14.9	0.3	1.9	−8.2	20.8
			12.0	0.3	5.4	−6.8	13.1
NaI	11.2	[28]	14.6	0.3	0.2	−8.3	22.4
			—	—	—	—	—
KF	8.6	[30]	12.2	0.3	6.2	−7.2	12.8
			—	—	—	—	—
KCl	6.1	[32]	11.0	0.3	8.6	−7.8	9.9
			8.1	0.3	7.5	−7.0	7.3
KBr	8.2	[32]	12.0	0.3	9.4	−7.6	9.9
			11.5	0.3	8.1	−6.9	9.9
KI	15.8	[32]	15.3	0.3	8.2	−7.7	14.5
			14.8	0.3	6.1	−7.0	15.4
RbF	9.5	[26]	10.4	0.3	5.2	−6.9	11.7
			—	—	—	—	—
RbCl	9.0	[32]	15.9	0.3	9.3	−7.6	13.9
			11.5	0.3	5.9	−7.2	12.5
RbBr	7.1	[32]	9.7	0.3	10.2	−7.5	6.7
			6.4	0.3	7.4	−6.9	5.6
RbI	7.5	[32]	12.0	0.3	11.3	−7.6	7.9
			7.8	0.3	10.2	−7.0	4.3
CsF	—		12.8	0.3	9.8	−6.2	8.9
			—	—	—	—	—

the potential energy. The Bridgman parameter can then be written

$$g = \tfrac{1}{3} - \tfrac{2}{3}\partial(\ln \theta_{res})/\partial(\ln r) + \tfrac{2}{3}\partial(\ln C_{111})/\partial(\ln r) + \tfrac{1}{3}\partial(\ln G_{res})/\partial(\ln r). \quad (14)$$

It may seem strange that the r-dependence gives a term $-\frac{1}{3}$ in equation (3) whereas it gives $+\frac{1}{3}$ in equation (14). This is explained, however, by the definition of γ in equation (2) [1]:

$$\gamma = rC_{111}/f \quad (15)$$

where f is a second-order derivative of the potential energy between nearest neighbours. If r had not been included in the definition of γ, we would have had an additional term $\frac{2}{3}$ in equation (3) since γ is squared in equation (2).

The calculated Bridgman parameter and the contributions from each term in equation (14) are given in table 8. We find a negative contribution to g from C_{111} and positive contributions from the other terms in equation (14) with the exception of the lithium salts where also θ_{res} gives a negative contribution.

When the contributions are summed, we find that the shell model always gives a higher value for g than the DD model does. This is consistent with our investigations in § 3, where the Grüneisen-mode parameters obtained with the shell model were usually greater than those obtained with the DD model. This suggests that the dispersion relations obtained with the shell model are more volume dependent than those obtained with the DD model. Since we found that none of our models worked well for the lithium salts, we shall not include these in the following discussion.

The calculated g-values range from 6.0 to 15.9. This range arises mainly from the last term in equation (14) which depends on the three-phonon scattering rate. As could be

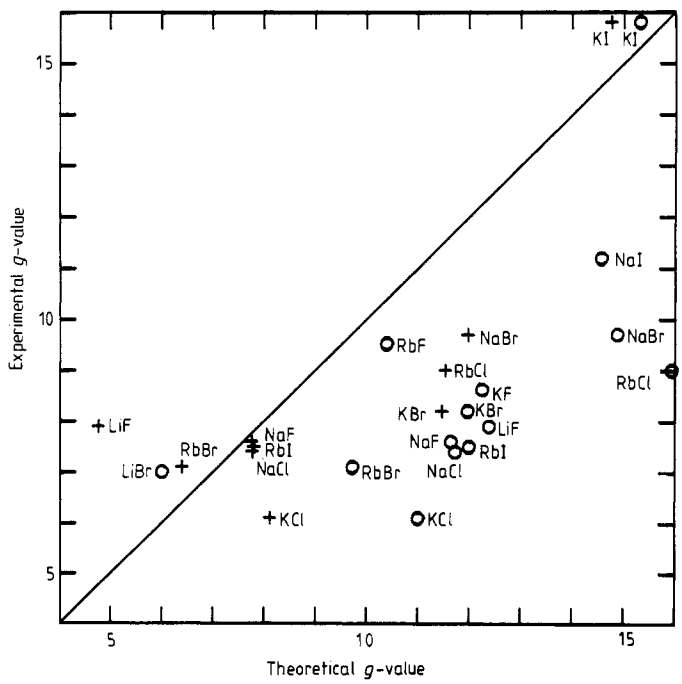

Figure 1. Plot of experimental values against theoretical values of the Bridgman parameter g: ○, shell model; + DD model.

expected, these scattering processes are sensitive to the shape of the dispersion relations which results in very different values for the contribution to g, not only from different crystals but also from different models applied to the same crystal.

The third term in equation (14), containing C_{111}, has nearly the same value for all alkali halides. This term does not contribute to the differences in g-values between crystals but it cannot be ignored in the calculations since the magnitude of g would then be in serious error.

The second term in equation (14) varies somewhat in the sequence of alkali halides and to some extent it modulates the large variations in the G_{res}-term. A high value of the G_{res}-term is often accompanied by a small value of the θ_{res}-term and vice versa.

Even though the results for the shell model and DD model differ in their absolute values, we find the same trends with both models. When comparing our calculated values with experimental values, we see in table 8 and figure 1 that the DD model gives better agreement with experiment.

6. Summary

We have calculated the dispersion relations with the shell model and the DD model. We find that the DD model gives good agreement with experiment for both the value of the frequencies and their volume dependence. The shell model does not give the correct value for the long-wavelength acoustic modes but it gives a better volume dependence than does the DD model.

The calculated values of the thermal conductivity at room temperature differ in the two models; to some extent, this is explained by different values of the third-order derivative of the potential energy of a pair of nearest neighbours. However, the calculated values are in most cases in good agreement with experiments.

The calculated volume dependence of the thermal conductivity gives a large variation in the values for the Bridgman parameter g which is also observed in experiments. The DD model also gives good agreement for the magnitude of g. The volume dependence of the number of three-phonon scattering processes is the main cause of the large variation between the g-values of the alkali halides. The contribution from the volume dependence of the anharmonic potential is approximately the same in all alkali halides and does not contribute to the differences in the g-values but it has to be included in order to obtain the correct magnitude of g.

Acknowledgments

I would like to thank Professor Arne Claesson for his interest and valuable support of this project. I would also like to express my gratitude to Dr Glen A Slack and Dr Bob Jones for many stimulating and clarifying discussions.

References

[1] Leibfried G and Schlömann E 1954 *Nachr. Akad. Wiss. Göttingen, Math. Phys.* IIa **71**
[2] Slack G A 1979 *Solid State Phys.* **34** 1 (New York: Academic)
[3] Ross R G, Andersson B, Sundqvist B and Bäckström G 1984 *Rep. Prog. Phys.* **47** 1347
[4] Roufosse M C and Jeanloz R 1983 *J. Geophys. Res.* **88** 7399

[5] Pettersson S 1987 *J. Phys. C: Solid State Phys.* **20** 1047
[6] Vaidya S N and Kennedy G C 1971 *J. Phys. Chem. Solids* **32** 951
[7] Sangster M J L and Atwood R M 1978 *J. Phys. C: Solid State Phys.* **11** 1541
[8] Sangster M J L, Schröder U and Atwood R M 1978 *J. Phys. C: Solid State Phys.* **11** 1523
[9] Jain J K, Shanker J and Khandelwal D P 1976 *Phys. Rev.* B **13** 2692
[10] Hardy J R and Karo A M 1979 *The Lattice Dynamics and Statics of Alkali Halide Crytstals* (New York: Plenum)
[11] Mahan G D 1986 *Phys. Rev.* B **34** 4235
[12] *Landolt–Börnstein New Series* Group III, vols 11, 1979 and 18, 1984 ed. H-K Hellwege (Berlin: Springer)
[13] Lowndes R P and Martin D H 1970 *Proc. R. Soc.* A **316** 351
[14] Lowndes R P and Rastogi A 1976 *Phys. Rev.* B **14** 3598
[15] Pettersen H E 1981 *J. Phys. Chem. Solids* **42** 1027
[16] Farr M K and Trevino S F *Proc. Conf. Neutron Scattering (Gatlinburg, TN) 1976* (Washington: ERDA) p 237
[17] Ernst G, Krexner G, Quittner G, Kress W, Buras B and Lebech B 1984 *Phys. Rev.* B **29** 5805
[18] Blaschko O, Ernst G, Quittner G, Kress W and Lechner R E 1975 *Phys. Rev.* B **11** 3960
[19] Mitra S S, Postmus C and Ferraro J R 1967 *Phys. Rev. Lett.* **18** 455
[20] Postmus C, Ferraro J R and Mitra S S 1968 *Phys. Rev.* **174** 983
[21] Ferraro J R, Mitra S S and Quattrochi A 1971 *J. Appl. Phys.* **42** 3677
[22] Shawyer M S and Sherman W F 1982 *Infrared Phys.* **22** 23
[23] Toulokian Y S, Kirby R K, Taylor R E and Lee T Y R 1977 *Thermal Expansion–Nonmetallic Solids Thermophysical Properties of Matter* vol 13 (New York: Plenum)
[24] Tosi M P 1964 *Solid State Phys.* **16** 1 (New York: Academic)
[25] Andersson S and Bäckström G 1987 *J. Phys. C: Solid State Phys.* **20** 5951
[26] Håkansson B 1988 private communication
[27] Håkansson B and Ross R G 1985 *Int. J. Thermophys.* **6** 353
[28] Håkansson B and Andersson P 1986 *J. Phys. Chem. Solids* **47** 355
[29] Sigalas I, Håkansson B and Andersson P 1985 *Int. J. Thermophys.* **6** 177
[30] Gummow R J and Sigalas I 1987 *J. Phys. C: Solid State Phys.* **20** L61
[31] Andersson P 1985 *J. Phys. C: Solid State Phys.* **18** 3943
[32] Slack G A and Ross R G 1985 *J. Phys. C: Solid State Phys.* **18** 3957